mmTag: A Millimeter Wave Backscatter Network

Mohammad Hossein Mazaheri
University of Waterloo
Waterloo, Ontario, Canada
mohammad.mazaheri@uwaterloo.ca

Alex Chen
University of Waterloo
Waterloo, Ontario, Canada
zihan.chen@uwaterloo.ca

Omid Abari
University of California Los Angeles
Los Angeles, California, United States
omid@cs.ucla.edu

ABSTRACT

Recent advances in IoT, machine learning and cloud computing have placed a huge strain on wireless networks. In particular, many emerging applications require streaming rich content (such as videos) in real time, while they are constrained by energy sources. A wireless network which supports high data-rate while consuming low-power would be very attractive for these applications. Unfortunately, existing wireless networks do not satisfy this requirement. For example, WiFi backscatter and Bluetooth networks have very low power consumption, but their data-rate is very limited (less than a Mbps). On the other hand, modern WiFi and mmWave networks support high throughput, but have a high power consumption (more than a watt).

To address this problem, we present mmTag, a novel mmWave backscatter network which enables low-power high-throughput wireless links for emerging applications. mmTag is a backscatter system which operates in the mmWave frequency bands. mmTag addresses the key challenges that prevent existing backscatter networks from operating at mmWave bands. We implemented mmTag and evaluated its performance empirically. Our results show that mmTag is capable of achieving 1 Gbps and 100 Mbps at 4.6 m and 8 m, respectively, while consuming only 2.4 nJ/bit.

CCS CONCEPTS

• **Hardware → Wireless devices**; **Wireless integrated network sensors**; • **Networks → Mobile networks**.

KEYWORDS

Backscatter communication; Internet of Things (IoT); mmWave communication; Low power; Wireless

ACM Reference Format:
Mohammad Hossein Mazaheri, Alex Chen, and Omid Abari. 2021. mmTag: A Millimeter Wave Backscatter Network . In *ACM SIGCOMM 2021 Conference (SIGCOMM '21), August 23–27, 2021, Virtual Event, USA.* ACM, New York, NY, USA, 12 pages. https://doi.org/10.1145/3452296.3472917

1 INTRODUCTION

With the advent of cloud computing, billions of devices need to send their data to the cloud, enabling new applications such as multi-user augmented reality, federated learning for IoT, and drone based video streaming for sporting events and disaster scenarios [33, 37, 38, 45, 52]. While these prospects sound exciting, the reality is that most of these applications require high data-rate wireless connectivity while having limited energy sources. Unfortunately, existing wireless networks can not support high data-rate while consuming low energy.

Millimeter wave (mmWave) technology promises to revolutionize wireless networks [32]. In fact, this technology has been declared as a central component in 5G and 6G cellular networks. mmWave wireless networks have two main advantages over traditional wireless networks. First, they provide much higher data-rates by operating in high-frequency spectrum (24GHz and above). Second, they can provide connectivity to many nodes simultaneously by performing space division multiplexing. Unfortunately, despite these advantages, existing mmWave networks have high power consumption which makes them unsuitable for applications with limited energy sources. For example, recent mmWave platforms developed by research communities such as OpenMilli, MiRa and the NI platform consume about 10-20 watts [2, 4, 47]. Commercial mmWave chipsets, such as the Qualcomm QCA9500, consume several watts [36]. The high power consumption of mmWave networks is due to the high power consumption of Radio Frequency (RF) circuits operating at mmWave frequencies. Unfortunately, this is a fundamental problem since the power consumption of RF circuits is proportional to their operating frequencies. Additionally, in contrast to traditional radios, mmWave radios require steerable directional antennas (i.e. phased arrays), which significantly increase the power consumption of these radios.

In this paper, we introduce mmTag, an ultra-low power mmWave network. mmTag's nodes consume only a few milliwatts, and hence they can be powered by a small battery or solar panel. mmTag enables the creation of low-power mmWave network by combining mmWave and Backscatter technologies. In particular, mmTag is a backscatter system which operates at mmWave frequencies. backscatter technology offers very low-power wireless communication by enabling nodes to piggyback their data on the radio frequency (RF) signals of other devices, instead of generating and transmitting their own signals. Eliminating the need for an active transmitter and power-hungry RF components has enabled backscatter devices to communicate on a very low energy budget. However, to build a backscatter system which operates in the mmWave frequency bands, mmTag must overcome multiple challenges.

a) Beam Alignment Challenge: Due to the high frequency nature of mmWave, these signals experience greater path loss than low frequency signals. Therefore, mmWave radios have to use directional antennas to focus their transmitted and received power into narrow beams to compensate for that loss. Communication between two mmWave nodes is only possible when their beams are

SIGCOMM '21, August 23–27, 2021, Virtual Event, USA

ACM ISBN 978-1-4503-8383-7/21/08…$15.00
https://doi.org/10.1145/3452296.3472917

well-aligned as shown in Figure 1. Moreover, when a node moves, it needs to search again for the best beam direction. Although past mmWave work has proposed different approaches and schemes for creating a directional beam and searching for the best beam direction [10, 16, 20, 30], they are not practical for backscatter devices for two reasons. First, in order to steer a beam, most existing schemes require phased array antennas. Unfortunately, phased arrays are costly and consume a significant amount of power which makes them impractical for backscatter devices [4, 26]. Second, and most importantly, all existing schemes require both nodes to transmit and/or measure the received signals. Backscatter devices can only reflect signals and can neither transmit nor measure the received signals. Therefore, to build a mmWave backscatter device, we need to design a beam searching scheme which does not require the device to have any transmitter or receiver. Moreover, we need to avoid using power-hungry mmWave hardware in our design, such as phased array antennas.

b) Self-Interference Challenge: Another challenge in designing a mmWave backscatter network is the self-interference problem. In particular, an Access Point (AP) device which communicates to backscatter nodes is required to transmit a query signal and listen to the node's response at the same time. This is a challenging task since the node's response is a modulated version of the transmitted signal, and hence it requires the AP to have a full-duplex radio to decode the backscatter signal. Unfortunately, full-duplex radios operating at mmWave frequencies, require complex analog and digital hardware and are not commercially available [40]. Therefore, we must develop a system which enables the AP to transmit and receive signals at the same time without complex and expensive hardware.

c) Mobility Challenge: The third challenge in building a mmWave backscatter network is dealing with mobility. In particular, communication must be possible regardless of the angle and orientation of the backscatter node. This is challenging since mmWave networks use directional antennas, as opposed to traditional wireless networks which use omni-directional antennas.

mmTag addresses these challenges. In particular, mmTag overcomes the beam alignment problem by building on the Van Atta technique [39], developing a directional backscatter node which modulates and reflects the received signal back in the direction of arrival, regardless of the incidence angle. This enables the node to have its beam always aligned toward the AP, even if they move. mmTag achieves this without using any costly or power hungry mmWave components such as amplifiers or phase shifters. Furthermore, mmTag uses the polarization property of antennas and introduces a novel feed network which solves the interference and mobility challenges. In particular, mmTag's nodes are able to change the polarization of the signal by 90° during reflection. This allows the AP to use antennas with orthogonal polarization for transmitter and receiver beams, and hence can easily separate the received signal from the transmitted signal regardless of the orientation of the nodes.

This paper makes the following contributions:

- We introduce mmTag, a mmWave backscatter network which enables high data-rate wireless links while consuming ultra-low power.

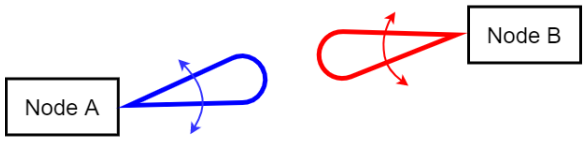

Figure 1: mmWave devices need to focus their energy into beams, and align them to establish a communication link.

- We design a novel backscatter node which modulates, changes polarization and reflects the received signal back in the direction of arrival, regardless of the incidence angle and without using any costly or power-hungry components.
- We built a prototype of mmTag and evaluated its performance empirically. Our results show that mmTag can achieve robust communication links with data-rates of 1 Gbps, 100 Mbps and 15 Mbps at a range of 4.6 m, 8 m, and 14 m, respectively .

2 BACKGROUND AND RELATED WORK

2.1 mmWave Communication

mmWave refers to high frequency RF signals in the range of 24 GHz to 100 GHz. At this frequency range, there is multi-GHz of unlicensed bandwidth available, 200x more than the bandwidth allocated to traditional wireless networks. The availability of this large bandwidth promises to enable wireless networks with orders of magnitude higher throughput than today's wireless networks [27]. Past work on mmWave communication mostly focuses on applications that require very high data-rate links, while using substantial energy and computing power. For example, [8] presented a system that enables high throughput links between server racks by using mmWave technology in data centers. There is also a significant amount of work on 5G networks which relies on mmWave technology [11, 32, 34]. mmWave technology has also been used for Virtual Reality to stream high data-rate video from PC to the VR headset [3, 9]. In contrast, this paper focuses on designing a mmWave backscatter network which enables low-power mmWave communication.

A major challenge in designing a mmWave network is that mmWave signals decay very quickly with distance, requiring mmWave radios to focus their power into very narrow beams in order to compensate for propagation losses [31]. These beams are typically created by using an array of antennas [24]. Luckily, since the antenna size is proportional to the wavelength, one can pack many mmWave antennas into a small area, creating a narrow beam. Although mmWave radios can compensate for the propagation loss using directional beams, a new challenge arises since communication is only possible when the transmitter's and receiver's beams are aligned [16]. Hence, mmWave devices need to continuously search the space for the best beam direction before establishing a communication link.

There is a vast literature on the area of mmwave beam alignment [3, 12, 16, 22, 35, 42, 46]. Most propose different techniques to speed up the beam searching process, enabling mmWave link

for mobile applications. However, these techniques require phased arrays to steer the beam electronically and search for the best beam alignment. Unfortunately, phased arrays are expensive to build and have high power consumption [4, 25, 26, 47]. Recent work has proposed a beam searching process without the use of phased array by exploiting channel blockage [26]. However, previous works require the node to have an active radio to transmit a signal or measure the received signal. Unfortunately, active radios significantly increase the power consumption of a wireless node, and are therefore not suitable for a backscatter design. In contrast, mmTag performs beam alignment using only passive components (i.e. without requiring any phased array, transmitter or receiver).

Finally, there is some preliminary work on designing a backscatter mmWave tag [17, 21]. However, this work focuses on sensing environment (such as humidity) rather than enabling high-data-rate, low-power communication links. Moreover, it does not support mobility truly since it does not work for all orientations of a tag. Concurrently to our work, the authors of [23, 41] proposed using mmWave backscatter for localization and intelligent transportation systems. However, their designs do not address modulation and self-interference problem, and hence can not be used for communication purposes. In contrast, mmTag focuses on designing a mmWave backscatter network which supports mobility and enables a low-power, high-data-rate communication link regardless of the location, angle and orientation of the node.

2.2 Backscatter Communication

Backscatter technology is the most energy-efficient wireless communication link [6, 18, 48, 50, 51]. A typical backscatter system consists of two parts: an AP and one or multiple backscatter nodes. The node communicates to the AP by backscattering instead of generating and transmitting its own signal. In particular, the AP transmits an RF signal to the node. The node replies to the AP by reflecting the signal using a simple modulation scheme. For example, in RFID the tag uses On-Off Keying (OOK) modulation where reflecting the reader's signal represents a '1' bit, and absorbing the signal represents a '0' bit. Due to its low-power consumption, this communication technology is well-suited for applications where battery replacement is challenging, or the battery life is expected to be long.

In recent years, RFID sensing systems have been designed in the research community to target a variety of applications ranging from food monitoring and smart homes to touch sensing and localization [14, 28, 29, 44]. There is also a significant amount of work focused on designing wireless networks for RFID tags [43]. However, existing RFID tags enable throughput of less than a Mbps. Recent work has proposed designing WiFi-based backscatter tags [5, 19, 51]. Their goal is to design backscatter nodes which communicate with WiFi devices to enable much higher throughput than traditional RFID tags, however their throughput is still very limited. For example, HichHike can only support 0.3 Mbps in the best case [48]. BackFi tries to solve the throughput problem of WiFi backscatter systems by using customized full-duplex radios. However, it can only support up to 5 Mbps at a short range of less than 1 meter (m) [5].

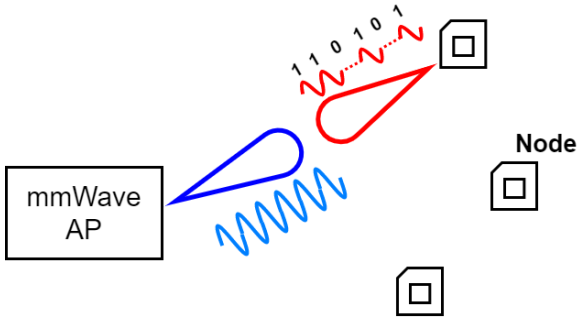

Figure 2: mmTag AP scans the space by steering its beam. When the AP's beam is toward a node, the node modulates and reflects the AP's signal back in the direction of arrival.

3 mmTAG OVERVIEW

mmTag is a low-power high-data-rate wireless network, achieved by operating at a mmWave frequency band while benefiting from the low-power nature of backscatter technology. As shown in Figure 2, mmTag is a system consists of one or more nodes which enable high-data-rate, low-power communication links to a mmWave AP. The AP uses directional antennas to create transmitting and receiving beams with orthogonal polarization. Then, it steers these beams together while transmitting a query signal. When the beams are facing toward a node, the node modulates, changes polarization and reflects the signal back to the direction of arrival (i.e. direction of the AP). The AP receives the backscattered signal, separates it from its own transmitted query signal, and decodes the node's message. Note, if the line-of-sight (LOS) path between the node and the AP is blocked, the AP chooses a non-line-of-sight (NLOS) path to communicate. The design of mmTag 's node does not require expensive or power hungry components such as phase array, DAC, mixer or baseband hardware. Moreover, it can be directly connected to a (GPIO) port of a microcontroller or an FPGA which is already available in user devices such as cameras, augmented reality (AR) headsets, or IoT devices providing high-data-rate connectivity.

Over the next few sections, we will first discuss how a mmTag node creates and steers a beam toward the AP without using active mmWave components and phased arrays. In particular, we explain how we can build a node which reflects the signal to the direction of arrival, regardless of the angle of incidence. Then, we explain how mmTag solves the interference problem and enables the AP to separate the backscattered signal from the query signal without using full-duplex hardware. Finally, we show how mmTag's nodes perform data modulation and communicate to AP for any angle and orientation.

4 BEAM ALIGNMENT CHALLENGE

As mentioned earlier, mmWave signals decay quickly as distance increases. Therefore, to achieve a reasonable communication range in a mmWave network, mmWave radios need to use directional antennas to focus their energy into a very narrow beam, compensating for the signal loss. Moreover, mmWave radios must be able to steer their beams to enable communication between mobile nodes, as shown in Figure 1. A steerable directional antenna is typically

implemented using a phased array. A phased array is an array of antennas, where each antenna is connected to a phase shifter. The phase shifter controls the phase of the signal on each antenna, which enables creating and steering a beam electronically. Finally, in order to find the correct direction for beam alignment, recent work has proposed different search techniques [10, 16, 22, 42, 46].

Similar to traditional mmWave networks, mmTag requires both the AP and nodes to use steerable directional beams and search for their correct direction. However, existing beam alignment schemes are not suitable for mmTag's nodes due to two reasons. First, all of these schemes require nodes to transmit and/or measure the received signals. However, a backscatter node does not have any transmitter or receiver radio; it can only reflect signals. Second, existing schemes require phased arrays which have high power consumption (a few watts) and are costly [4, 26]. In the following subsections, we explain how we build on the Van Atta technique to solve the beam alignment problem of backscatter nodes without using any active block (such as phased arrays, transmitter or receiver) in mmTag's design.

4.1 Principles of Antenna Array

Before explaining the solution, we first provide some principles about antenna arrays. An antenna array is an array of N antennas, spatially separated by distance d. In an antenna array, the signal received by the n^{th} antenna element can be written as:

$$x_n = x_0 \cdot e^{-jK_0 \cdot n \cdot d \cdot sin(\theta)};\ n \in [0 : N-1], \tag{1}$$

where K_0 is the free space wave number and θ is the angle of signal arrival. In a typical antenna array, $d = \frac{\lambda}{2}$ and $K_0 = \frac{2\pi}{\lambda}$, where λ is the wavelength of the signal. We can simplify Eq. (1) to:

$$x_n = x_0 \cdot e^{-j\pi \cdot n \cdot sin(\theta)};\ n \in [0 : N-1] \tag{2}$$

This equation shows that if we want to receive a signal from a specific direction (θ), we can multiply the received signal at each antenna with $e^{j\pi.n.sin(\theta)}$ and then sum them. Similarly, this equation implies that if we want to use an antenna array to transmit a signal to a specific direction (θ), we need to feed the following signal to each antenna:

$$y_n = y_0 \cdot e^{+j\pi.n.sin(\theta)};\ n \in [0 : N-1] \tag{3}$$

where n is the antenna number, and y_0 is the signal fed to the first antenna. Note that the only difference between Eq. (2) (i.e. equation for receiving from direction θ) and Eq. (3) (i.e. equation for transmitting to direction θ) is the inverted signal phases.

4.2 Passive Beam Searching

Now, we explain how we solve the beam alignment problem in mmTag's nodes. The backscatter nodes require having two beams, one for receiving the signal from the AP and one for reflecting the signal back to the AP. Due to the symmetry of forward and backward channels in backscatter communication, the correct direction for these two beams are the same. Said differently, the nodes need to reflect the signal back towards the direction of arrival. Now, the question here is how can we build a passive reflector which reflects the received signal back in the direction of arrival, regardless of the arrival (incidence) angle. Note, this is different from a typical reflector (such as mirror) which does this only when the angle of incidence is 0 degree.

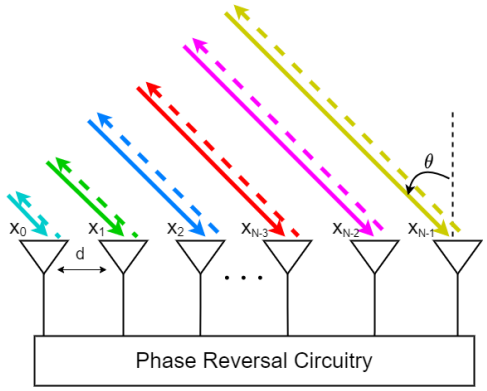

(a) Active Approach

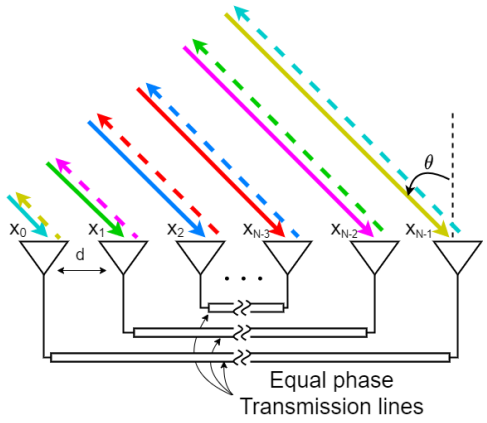

(b) Passive Approach (mmTag)

Figure 3: Directional reflectors using two different approaches. The solid arrows show the received signal and the dashed arrows show the reflected signal of each antenna element. In (a) each antenna reflects its own received signal, while in (b) each antenna reflects the signal received by its mirrored antenna.

Using principles of an antenna array described in Section 4.1, we can show that one approach to build such a node is to design an antenna array where each antenna element reverses the phase of the received signal, reflecting it back from where it came. This would give us a backscatter node which reflects the signal back to the same direction as the incidence angle for any incidence angle. Now, the next question deals with how we can reverse a phase of the signal.

A common way to reverse the phase of a signal is to use the phase reversal circuits, as shown in Figure 3(a). However, these circuits are complex and power hungry, hence are not suitable for a passive backscatter node. To solve this problem and build a mmWave backscatter node which reflects to the same direction as arrival direction, we design a device using Van Atta which is a

technique for building reflector array [39]. As shown in Figure 3 (b), we use an array of antennas where each antenna is connected to its mirrored antenna using a transmission line.[1] Therefore, each antenna receives a signal and passes it to its mirrored antenna to reflect it. Now, if we carefully design the transmission lines to have the same phase shifts between antenna pairs, the reflected signal from n_{th} antenna element will be:

$$y'_n = e^{j\phi} \cdot x_{N-n-1};\ n \in [0 : N-1] \tag{4}$$

where x_{N-n-1} is the signal received by the $(N-n-1)^{th}$ antenna element, and ϕ is the phase shift caused by the transmission lines. Then using Eq.1, we can write:

$$\begin{aligned} y'_n &= e^{j\phi} \cdot x_0 \cdot e^{-j\pi(N-n-1)\cdot sin(\theta)} \\ &= e^{j\phi} \cdot e^{-j\cdot\pi\cdot(N-1)\cdot sin(\theta)} \cdot x_0 \cdot e^{+j\cdot\pi\cdot n\cdot sin(\theta)} \\ &= y'_0 \cdot e^{+j\cdot\pi\cdot n\cdot sin(\theta)};\ n \in [0 : N-1] \end{aligned} \tag{5}$$

By comparing Eq.5 with Eq.3, we can see that mmTag's node creates a directional reflector which reflects the signal back to the direction of arrival regardless of incidence angle. Therefore, this design enables the node to reflect the signal back to the same path through which the signal has arrived from the AP. Note, the path between the node and the AP can be either LOS or NLOS. mmTag uses this design to solve the beam alignment problem of backscatter nodes without using any active components.

4.3 Data Modulation

So far we have explained how mmTag solves the beam alignment problem. However, to enable the node to send data to the AP, it must first modulate the signal before reflecting it back to the AP. Note, the backscatter node needs to do this using a simple and low-power approach. One naïve solution is to use a similar technique as traditional backscatter systems such as RFID. In these systems, an RF switch is used to connect the antenna to the ground plane. When the switch is on, the antenna is connected to the ground and does not reflect the query signal, and when the switch is off, the antenna reflects the query signal. Unfortunately, this simple approach does not work for mmWave backscatter nodes because RF switches have high leakage at mmWave frequencies when the switch is off, and hence the the signal reflection does not change much by turning the switch on or off.

To solve this problem, we use Single Pole Double Throw (SPDT) switches, where the input port of each SPDT is connected to an antenna, and the two output ports of SPDTs are connected to two transmission lines with different length, as shown in Figure 4. The length of these lines are carefully chosen such that when the antenna is connected to line L1, the antenna is tuned, and hence it resonates and reflects the signal back. On the other hand, when the the antenna is connected to the line L2, the antenna is not tuned and therefore does not reflect the signal back. Therefore, by turning the switches on or off, the node can change the amplitude of the reflected signal. Note, this technique does not impact on the phase of the signal and hence the reflected signal still goes back to the arrival direction. Finally, by connecting the data stream to the control line of switches, a mmTag's node can modulate the reflected signal and

[1]Transmission lines can be simply implemented by copper strips on a PCB board.

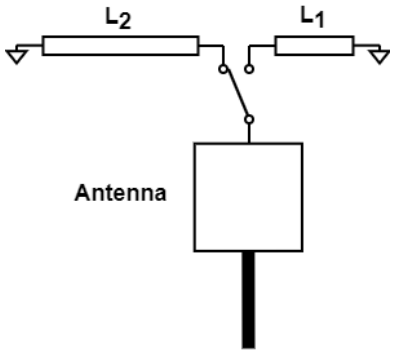

Figure 4: Data Modulation. mmTag's node uses a SPDT to switch between two transmission lines with different length. This allows the node to modulate the signal.

embed its data. For example, when the data bit is '1', the switches are in 1 positions and the amplitude of the reflected power is high at the AP. When the data bit is '0', the switches are in 0 position and the AP receives no reflected signal from the backscatter node. As a result, the AP can simply decode the node's data using Amplitude Shift Keying (ASK) demodulation. Although ASK is not as spectral efficient as complex modulations such as QAM, it is very attractive for backscatter devices since it does not require complex hardware with high power consumption. Furthermore, in Section 7 we will discuss how mmTag exploits the directional property of mmWave communication to enable the spacial frequency reuse and improve the spectrum usage.

5 SELF INTERFERENCE CHALLENGE

So far, we have explained how we build a backscatter node which modulates and reflects the query signal back to the AP without using active and power hungry components. Now, the question is how the AP can separate the node's signal from its own signal. Note, this is very challenging since the the reflected signal is much weaker than the query signal. In particular, when the node is far from the AP, the reflected signal is orders of magnitude smaller than the AP's query signal. Unfortunately, the AP can not amplify the reflected signal since the self-interference signal also gets amplified, results in the saturation of AP's receiver.

One might imagine that since mmWave radios use directional antennas, the leakage between the transmitter and receiver beam should be negligible. However, past work shows that there still exists a significant amount of leakage between their transmitter and receiver beams [3]. This leakage is problematic since it limits the amplification gain of the AP's receiver, and hence it significantly limits the operating range of our system. One possible approach to solve this problem is to use a full-duplex radio in the AP side to enable the AP to cancel the strong interference coming from its own transmission to the receiver. In fact, past backscatter systems (such as RFID) which operate at lower RF bands use these technique to reduce the self-interfering problem. However, full-duplex radios operating at mmWave frequencies are not commercially available.

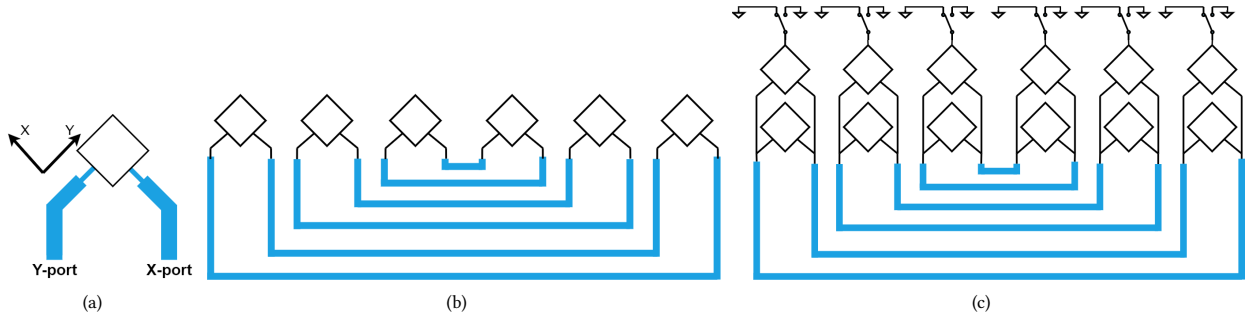

Figure 5: mmTag's node design. (a) our single element patch antenna with two port which enables operating in two different polarization. (b) our feed network design which enables the node to change the polarization of the received signal and then reflect it. (c) final design of mmTag where each antenna is connected to a switch to modulate the reflected signal.

Furthermore, the mmWave full-duplex radios proposed in the literature require complex and expensive hardware and do not perform beam searching which is essential for mobile applications [40].

5.1 Polarization Conversion

To solve the self-interference problem, we use the polarization property of antennas. In general, antennas have different polarization. In order for two antennas to hear each other, their polarization must be aligned. Said differently, if two antennas use orthogonal polarization, they will not hear each other's signal. Hence, mmTag's AP solves the interference problem by using antennas with orthogonal polarization for its transmitter and receiver. Although this solves the self-interference problem, it causes a new problem; the AP does not hear the the node's signal either. Therefore, for this idea to work, the node must change the polarization of the signal before reflecting it back. In other words, if the AP transmits the signal in polarization A, the node should receive this signal, and reflect it back in polarization B, which is orthogonal to polarization A. Note, since the other reflectors in the environment do not change the signal polarization, and only the signal reflected by the node has experienced polarization change, the AP can easily separate the node's backscattered signal from other signals including its own transmitted query signal.

In order to change the polarization of the backscatter signal, we design a patch antenna which has two ports as shown in Figure 5(a). Each port corresponds to one polarization. In particular, if we feed a signal into port X, the polarization of the radiated wave would be in X direction and if we feed the signal into the other port (port Y), the polarization would be in Y direction. This design enables us to have an antenna which can operate in two different orthogonal polarization depending on which port is used. Next, we use multiple versions of these patch antennas and build a reflector array as explained in Section 4. However, since each antenna has two ports, we connect port X of each antenna to port Y of its mirrored antenna as shown in Figure 5(b). This design enables the node to change the polarization of the received signal from X direction to Y direction and vice versa, as shown in Figure 6(a).

So far, we have explained how the node can change the signal polarization from X direction to Y direction and vice versa. However, depending on the orientation of the node, the arrival signal might be aligned to neither X nor Y direction as shown in Figure 6(a). Therefore, we need to have a design which converts any incoming polarization to its orthogonal. To solve this problem, we found that if we design the transmission lines to have 180° phase difference, the node converts any incoming polarization to its orthogonal. To consider why this works, consider an example shown in Figure 6(b). In this example, if we exchange the value of X and Y and rotate X by 180°, the reflected signal will be orthogonal to the received signal. Therefore, our design enables the node to change the signal polarization to its orthogonal one and reflect it back regardless of the angle or orientation of the node respect to the AP. It is worth mentioning that in most backscatter systems, nodes have linear polarization and therefore their readers have to use

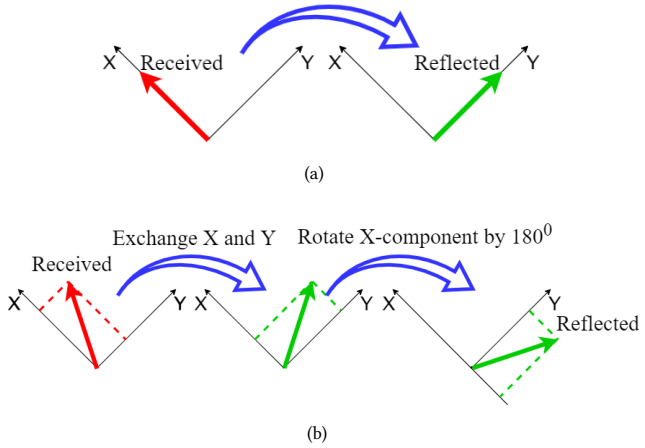

Figure 6: Polarization Conversion. (a) if the polarization of the received signal is in X direction, mmTag's node change it to Y direction and reflect it. (b) if the polarization of the received signal has an arbitrary direction, mmTag's node change it to the orthogonal direction by exchanging the signal of X and Y port and performing a 180 degree phase shift on X.

circularly polarized antennas to enable robustness to orientation changes. However, mmTag's nodes do not use linear polarization and work with any orientaiton. Therefore, this enables us to use linear polarization at the reader side and still provide robustness to orientation changes. Finally, to provide higher radiation gain and improve the communication range, instead of using a single patch antenna for each element, we use two cascaded patch antennas as shown in Figure 5(c). The cascaded patch antennas have around 60 degree beamwidth, and hence there is no need for beam alignment in the elevation plane.

In summary, mmTag's node uses a passive beam alignment technique to hear a query signal from the AP. It then modulates the signal, changes its polarization, and reflects it back toward the direction of the This enables a mmTag node to communicate with the AP without requiring complex and power hungry hardware such as full-duplex radios at the AP and phased arrays at the node.

6 LINK BUDGET ANALYSIS

In previous sections, we have described different parts of our design. Here, we perform a link budget analysis for mmTag. For our analysis, we make the following assumptions. AP transmission power is 12 dBm which is in accordance with the FCC rules [1]. The receiver antenna has 20 dBi gain. The Low Noise Amplifier (LNA) at the receiver side provides 20 dB gain. We also consider 4 dB loss for cables and connections. Finally, each cascaded patch antenna on the mmTag's node provides 8 dBi gain and it has around 1.5 dB loss due to the transmission lines used for the beamforming.

Considering these parameters, we calculate the power of node's signal at the AP side for different distances between the AP and the node. Figure 7 shows the result of this analysis for different size of the node's array. The figure shows that as the number of antenna elements increases, mmTag can support longer ranges and higher datarates. Therefore, depending on the range, data-rate and size constraints of an application, one can design a mmTag's node with different number of antenna elements. When the node has 6 elements (where each element is two cascaded patch), the node's signal power is -70 dbm and -82 dBm at 5 m and 10 m, respectively. Note, considering ASK modulation and BER of $10^{-}3$, these signal powers are high enough to support 1.5 Gbps and 96 Mbps at 5 m and 10 m, respectively.

7 SUPPORTING MULTIPLE NODES

So far, we explained how a single mmTag node communicates to an AP. In this section, we explain how mmTag enables multiple nodes to communicate to an AP. mmTag uses a combination of spacial-division and time-division multiplexing to enable communication to multiple nodes. In the following section, we discuss them in more details.

a) Spatial Division Multiplexing (SDM) In this technique, the AP creates a narrow beam and scans the environment while transmitting a query signal. During this time, each node sends a predefined packet which is used by the AP to identify and find the direction of each node. Once the AP finds the direction of all nodes, it establishes communication links to them by focusing its beam toward them in a round-robin manner. This approach enables the AP to support all nodes. However, it worth mentioning that if an application requires supporting multiple nodes concurrently, one can simply use MIMO beamforming architecture at the mmTag AP which enables creating multiple independent beams, each directed toward a different node.

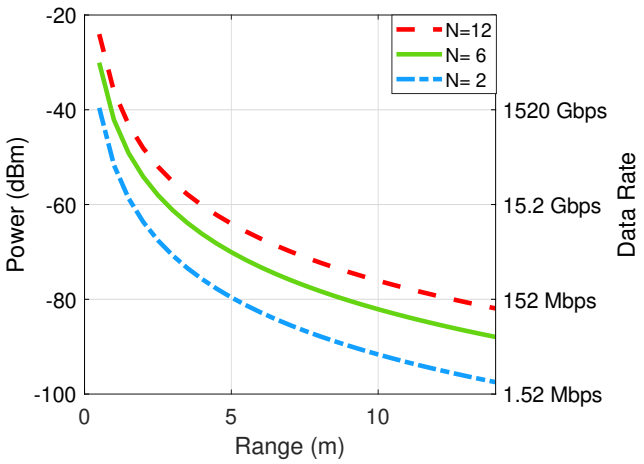

Figure 7: Link Budget Analysis

b) Time Division Multiplexing (SDM) In scenarios where a large number of nodes are connected to a single AP, there is a chance that two or more nodes are located in the same direction respect to the AP. Therefore, their reflected signals collide and the AP can not decode them. To avoid this, mmTag employs Time Division Multiplexing. In this scheme, the AP assigns a time slot to each node to send its data while the other nodes stay silent. The AP and nodes can use low-power, low-data-rate radios, such as Bluetooth, to exchange their control information.

8 IMPLEMENTATION

In this section, we describe the implementation of mmTag's node and the mmWave AP's setup.

We design mmTag using ANSYS HFSS software. The node is then fabricated on PCB using standard Rogers 4835 material with 0.18 mm thickness, as shown in Figure 8. The node is integrated with ADRF5020 SPDT switches that have very low power consumption. This is the only mmWave IC used in our node, making the design simple and low-cost. Our design is tuned to cover the whole 24 GHz mmWave ISM band with 250 MHz bandwidth. However, the same method and design approach can be used to design a mmTag's node operating at higher frequencies (such as 60 GHz) where 2 GHz of bandwidth is available. As long as the ratio of bandwidth to center frequency (fractional bandwidth) is less than 10%, the proposed beam alignment technique works. The size of mmTag's node is 6×5 cm, including 6 antenna elements (where each is two cascaded path). The node creates a directional beam with 12 degree beam width. Note, our design can be easily tuned to higher frequency bands (such as 60 GHz) which results in even smaller antennas.[2] For the mmWave AP, we use a signal generator and a spectrum

[2]The higher the frequency, the shorter the wavelength, and therefore the smaller the antennas.

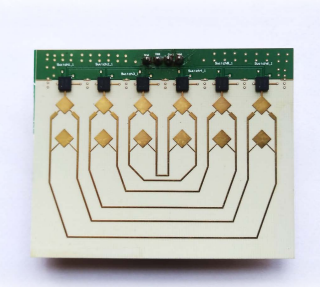

Figure 8: Our mmTag's node fabricated on PCB. The dimension of the node is only $6 \times 5\ cm^2$ (i.e. smaller than a credit card).

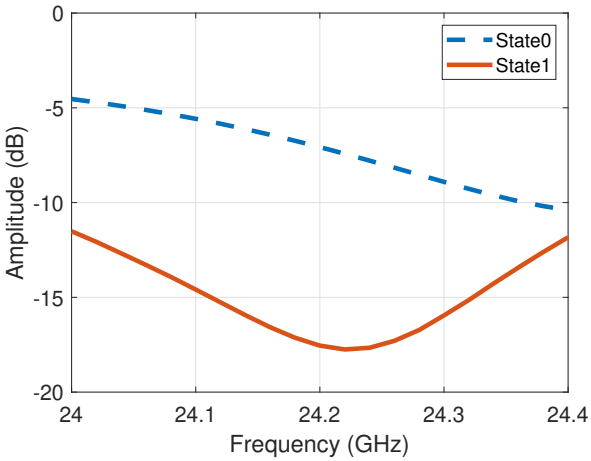

Figure 9: S11 coefficient of a node's antenna element for both states of the switch. In one state, antenna has low S11 at the carrier frequency of 24 Ghz and hence it receives and reflects. In the other state, the antenna's S11 is high and hence it does not receive nor reflect.

analyzer, and connect them to directional antennas to transmit and receive 24 GHz signals. The AP's average transmission power (including the transmitter antenna's gain) is 12 dBm. Note, the peak transmission power can be higher if the AP performs duty cycling. We use an LNA with 25 dB gain for the AP's receiver.

9 EVALUATION

We evaluated the performance of mmTag in different locations, angles, and orientations. We ran experiments in an indoor environment where shelves and tables were present around the measurement area.

9.1 Microbenchmarks

Switched Antenna Performance We first evaluate our node's ability in modulating and reflecting a signal. As described in Section 4.3, we use low power SPDT switches to switch the node between two modes: reflective and non-reflective. Figure 9 shows

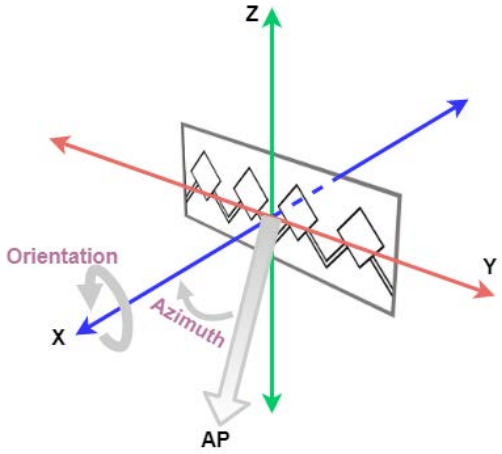

Figure 10: Evaluation Scenarios. We empirically evaluated mmTag for different ranges, orientations and angles of the node respect to the AP.

the result of our evaluation. The figure shows the S11 of a single element of the node when its switch is in state 0 and state 1. When the switch is state 1, S11 is less than -15 dB at the carrier frequency. This implies that antenna is tuned. Therefore, in this mode, the antenna works properly and the node receives the mmWave signal from the AP and reflects it back in the same direction. On the other hand, when the switch turns to state 0, the figure shows the S11 is as high as -5 dB at the carrier frequency. Such a high S11 means that the antenna is not tuned. Therefore, the antenna does not work in this mode and it does not receive nor reflect the AP's signal. This evaluation confirms that our node is able to modulate and reflect the mmWave signal.

Passive Beamforming: As mentioned in Section 4, mmTag's node reflects back the signal toward the AP, regardless of the incidence angle. Here, we empirically evaluate the nodes ability in performing this. To do so, we run an experiment where we place the node at 1 m from the AP and rotate the node in the azimuth direction as shown in Figure 10 while measuring the power of the reflected signal. Figure 11 shows the normalized received power from the node versus rotation angles. For comparison, we also show the received power if we were using a wide-beam single antenna (yellow plot) or a fixed-beam antenna array (red plot) instead of our design. The figure shows that our design experiences much lower power loss in the reflected signal. This implies that the node can perform passive beam forming toward the AP, regardless of its angle with respect to the AP.

Polarization Conversion: Here, we evaluate if using orthogonal polarization helps mmTag to solve the self-interference problem of the AP. We ran an experiment where the AP is continuously transmitting a query signal while also measuring the power of the received signal (i.e. self-interference) at the receiver antenna. We performed this experiment for two scenarios: (a) the AP used antennas with orthogonal polarization for transmitting and receiving, and (b) the AP used antennas with the same polarization for transmitting and receiving. Our results shows that the power of

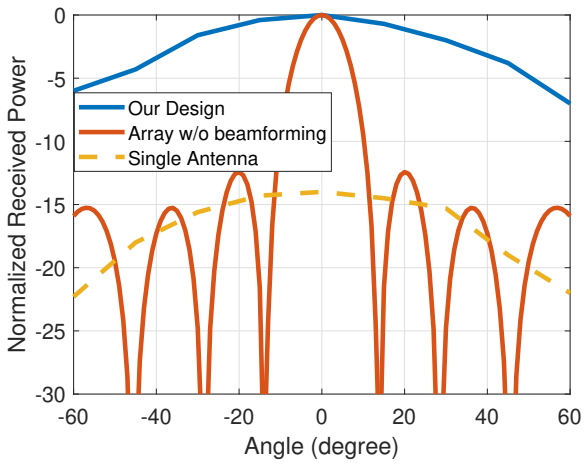

Figure 11: mmTag's Passive beamforming performance. mmTag's node reflects the signal back to the direction of the AP while experiencing minor loss across different angles respect to the AP. The figure also shows that the loss would be much higher if a fixed-beam array or a single antenna was used instead of mmTag's design.

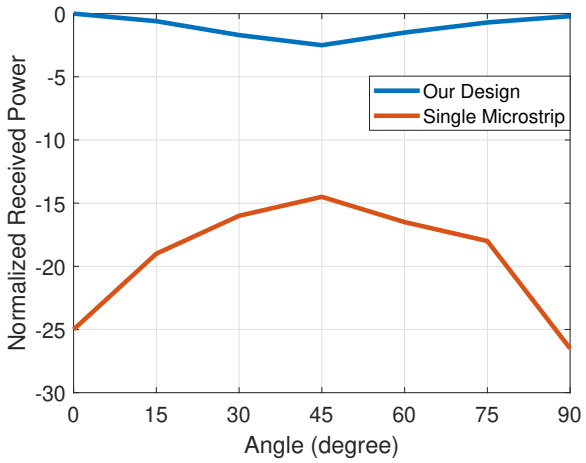

Figure 12: mmTag's polarization conversion performance. mmTag's node converts the polarization of a signal to its orthogonal polarization with minor loss for any orientation of the node. The figure also shows that the loss would be much higher if a typical patch antenna was used instead of mmTag's design

self-interference signal in the first scenario is 31 dB lower than in the second scenario. This result implies that mmTag can significantly reduce the impact of the self-interference problem, resulting in a significant improvement in the operating range.

However, for this approach to work, the node must always be able to change the polarization of the signal. Next, we evaluate the performance of the mmTag node in changing the signal polarization for different orientation angles. As discussed in Section 5, mmTag uses a novel antenna and feed network design which converts any incoming signal polarization to its orthogonal, and hence, it can communicate to the AP regardless of orientation of the node. To evaluate this capability, we run an experiment where we place the node at 1 m from the AP. We then measure the power of the reflected signal from the node at the AP, while we rotate the node around its x-axis as shown in Figure 10. The normalized received power is shown in Figure 12. For comparison, we also plot the received power if we were using a typical patch antenna instead of our design. This result shows that mmTag's node experiences less than 3 dB loss across all different rotation angles. On the other hand, if we were just using a typical patch antenna which does not change the polarization, we would experience much higher loss. This result implies that the node can reflect the signal and enable robust communication to the AP, regardless of its orientation.

9.2 mmTag's Range Performance

Next, we evaluate the performance of mmTag as a communication link for different distances of a node from the AP. In this experiment, the AP transmits a query signal to the node and measures the power of the signal reflected back from the node. Figure 13 shows the result of this experiment for different distances between the node and AP. The figure also shows the noise floor of the AP for different bandwidths as well as the node's maximum data-rate for some ranges.[3] Note, there is currently 250 MHz of ISM band available at 24 GHz which can support up to 125 Mbps. Therefore, in order to evaluate our system for higher data-rates, the received powers are measured empirically and the corresponding data-rates are computed by substituting the power measurements and the noise floor into standard data-rate tables based on the ASK modulation and BER of 10^{-3}, which is a typical BER for most backscatter systems. [4] Note, mmTag's BER can be improved by increasing the number of antenna elements on the node, or operating at lower datarate or shorter range. Our results show that mmTag provides more than 1 Gbps data rate when the node is less than 4.65 m from the AP. The figure also shows that increasing the distance reduces the node's signal power. However, mmTag can still provide 100 Mbps and 10 Mbps at even 8 m and 14 m, respectively. Note, our empirical results are based on transmit power of 12 dbm, including the antenna gain. In order to achieve longer range or higher data-rate, one can duty cycle the transmission of the query signal while keeping the average transmission power at 12 dbm which complies with FCC regulation [1]. Figure 13 shows the results when the query signal is 10% duty cycled. In this case, mmTag achieves the maximum data rate of 1 Gbps even at 8 m distance. Finally, it is worth mentioning that our current node design has 6 antenna elements. The range and and data-rate can be increased further by designing a node with more elements.

[3] mmTag's AP uses CMD298C4 LNA which has Noise Figure (NF) of 1.4 dB. The AP's noise floor is computed based this Noise Figure and thermal noise at the room temperature (i.e.300 K).
[4] ASK modulation requires SNR of 7 dB to achieve BER of 10^{-3} [13].

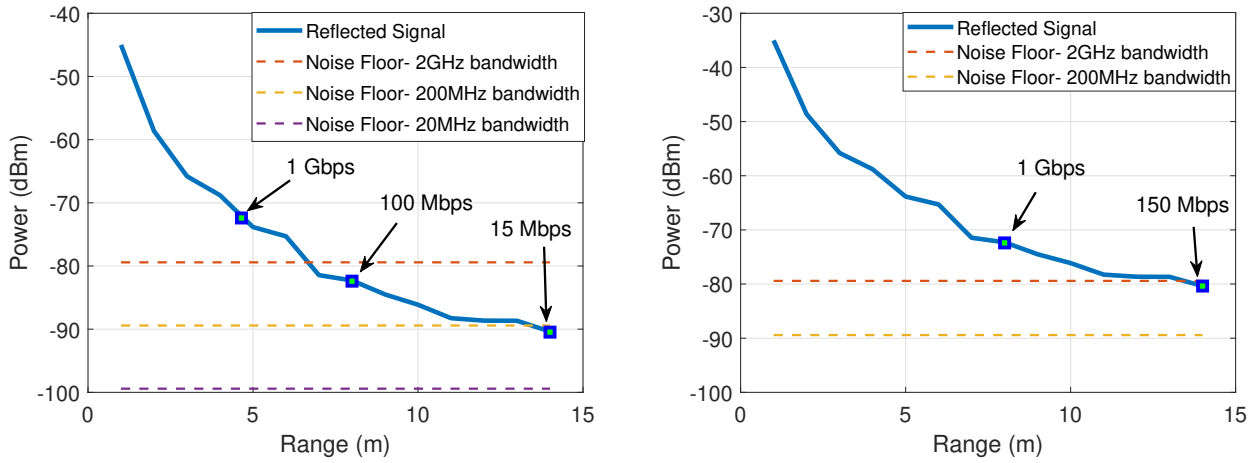

Figure 13: mmTag range performance. The figure shows the power of tag's signal measured at the AP versus distance between the node and the AP for (a) AP is continuously transmitting the query signal and (b) AP is performing 10% duty cycling. The figure also shows the noise floor for different AP bandwidth as well as corresponding data rates for some signal powers.

Systems	Maximum Range	Data-rate	Energy efficiency (nJ/bit)
mmTag	**14 m**	**100 Mbps** (at 8 m)	**2.4**
mmX [26]	18 m	100 Mbps	11
Mira [4]	100 m	1 Gbps (at 18 m)	11.6
WiFi (802.11n) [7, 15]	50 m	120 Mbps (at 18m)	17.5
Bluetooth	10 m	1 Mbps	29
WiFi backscatter [49]	6 m (to TX)	300 Kbps	0.11 (simulation)

Table 1: Comparison of mmTag with other wireless systems

9.3 mmTag's System Performance

So far, we have evaluated the performance of mmTag for different distances while it has been facing the AP. Next, we evaluate mmTag's performance for different distances and orientations together. Figure 14 shows the received power from the node for different distances and angles. The figure shows that mmTag can achieve SNRs higher than 7 dB for all scenarios. The figure also shows the corresponding bit error rate (BER) for each SNR. This result implies nodes can communicate to the AP successfully, regardless of their location, angle or orientation with respect to the AP. Therefore, we conclude that mmTag supports mobile applications.

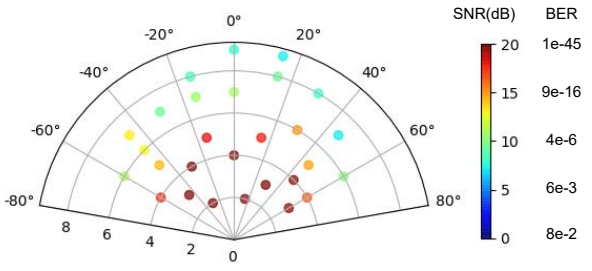

Figure 14: mmTag System Performance. mmTag enables high-SNR communication link between the AP and nodes for different scenarios (i.e. different range, orientation and angle of the node respect to the AP.)

9.4 mmTag's Power Consumption

A key promise of mmTag is that it enables low-power mmWave communication for devices with limited energy resources. Here, we evaluate the power consumption of mmTag's node. The design of mmTag's node is mostly using passive traces and transmission lines, namely the only components used in the design are six SPDT switches. Our measurement shows that the mmTag's node consumes 2.4nJ/bit. It is worth mentioning that mmTag's node design does not need a DAC, mixer or baseband hardware, and it receives a bit stream by directly connecting it to a (GPIO) port of a microcontroller or an FPGA which is already available in the user device such as a camera, an Augmented Reality (AR) headset, or an IoT device.

10 DISCUSSION

In this section, we compare mmTag with existing wireless systems such as WiFi, Bluetooth, WiFi backscatter and other mmWave platforms. Specifically, we compare these systems in terms of power consumption, throughput, and range. Table 1 shows the results of this comparison.

Past mmWave platforms such as MiRa cost a few thousand dollars and consume more than 10nJ/bit. On the other hand, mmTag is low cost and consumes only 2.4nJ/bit. It is worth mentioning that past mmWave platforms provide multi-Gbps throughput and long range communication links which make them suitable for applications with substantial energy resources available. In contrast, mmTag targets applications with limited energy sources.

In comparison to WiFi, the main advantage of mmTag is that it consumes orders of magnitude lower power. Furthermore, mmTag utilizes mmWave spectrum (24 GHz) and hence it will remove a huge strain from today's WiFi spectrum. Finally, note that the reported WiFi bit-rate performance is for an ideal scenario. In fact, most of today's WiFi networks have much lower performance since their spectrum is overloaded.

In comparison with Bluetooth and WiFi backscatter, mmTag provides a much higher data-rate while having similar power consumption. Specifically, Bluetooth and WiFi backscatter provide only 1 Mbps and 300 Kbps, respectively, which are not sufficient for many applications. On the other hand, mmTag provides 1 Gbps and 100 Mbps at 4.6m and 8m respectively, making it suitable for many low-power applications which require high-data-rate links.

11 CONCLUSION

In this paper, we present mmTag, a mmWave backscatter communication system which enables a data-rate similar to other mmWave networks with power consumption similar to backscatter networks. Today's backscatter networks (such as RFID and WiFi baskscatter) enable low-power wireless communication which is very attractive for devices with limited energy resources. However, backscatter networks provide very limited data-rates which are not suitable for many emerging applications. On the other hand, existing mmWave network enable very high-data-rate links but have high power consumption. In this paper, we developed and evaluated a backscatter network which operates in the mmWave spectrum. Hence, it benefits from both low power consumption of backscatter networks and large bandwidth available at mmWave frequencies. Our results show that mmTag provides Gbps communication links with nodes that consume only 2.4nJ/bit. We believe mmTag enables wireless links for many emerging applications which deliver content in real-time while having limited energy resources available.

ACKNOWLEDGMENTS

We acknowledge the CMC Microsystems for supporting and providing software access. We also thank the Natural Sciences and Engineering Council of Canada (NSERC) for partial funding for this project. We thank CIARS group for letting us use their test equipment and laboratory services. Finally, we appreciate the anonymous reviewers, and our shepherd, Aaron Schulman, for their helpful feedback

REFERENCES

[1] [n.d.]. Federal Communications Commission. Title 47, code forfederal regulations.
[2] 2015. 71-76 GHz Millimeter-wave Transceiver System. National Instruments.
[3] Omid Abari, Dinesh Bharadia, Austin Duffield, and Dina Katabi. 2017. Enabling high-quality untethered virtual reality. In *14th {USENIX} Symposium on Networked Systems Design and Implementation ({NSDI} 17)*. 531–544.
[4] Omid Abari, Haitham Hassanieh, Michael Rodreguiz, and Dina Katabi. 2016. Poster: A millimeter wave software defined radio platform with phased arrays. In *Proceedings of the 22nd Annual International Conference on Mobile Computing and Networking*. 419–420.
[5] Dinesh Bharadia, Kiran Raj Joshi, Manikanta Kotaru, and Sachin Katti. 2015. Backfi: High throughput wifi backscatter. *ACM SIGCOMM Computer Communication Review* 45, 4 (2015), 283–296.
[6] Colby Boyer and Sumit Roy. 2013. —Invited paper—Backscatter communication and RFID: Coding, energy, and MIMO analysis. *IEEE Transactions on Communications* 62, 3 (2013), 770–785.
[7] Cisco. [n.d.]. *Wireless Mesh Constraints*. https://www.cisco.com/c/en/us/td/docs/wireless/technology/mesh/7-3/design/guide/Mesh/Mesh_chapter_011.pdf
[8] Yong Cui, Shihan Xiao, Xin Wang, Zhenjie Yang, Shenghui Yan, Chao Zhu, Xiang-Yang Li, and Ning Ge. 2017. Diamond: Nesting the data center network with wireless rings in 3-d space. *IEEE/ACM Transactions On Networking* 26, 1 (2017), 145–160.
[9] Mohammed S Elbamby, Cristina Perfecto, Mehdi Bennis, and Klaus Doppler. 2018. Toward low-latency and ultra-reliable virtual reality. *IEEE Network* 32, 2 (2018), 78–84.
[10] Mohammed E Eltayeb, Ahmed Alkhateeb, Robert W Heath, and Tareq Y Al-Naffouri. 2015. Opportunistic beam training with hybrid analog/digital codebooks for mmWave systems. In *2015 IEEE Global Conference on Signal and Information Processing (GlobalSIP)*. IEEE, 315–319.
[11] Zhen Gao, Linglong Dai, De Mi, Zhaocheng Wang, Muhammad Ali Imran, and Muhammad Zeeshan Shakir. 2015. MmWave massive-MIMO-based wireless backhaul for the 5G ultra-dense network. *IEEE Wireless Communications* 22, 5 (2015), 13–21.
[12] Yasaman Ghasempour, Muhammad Kumail Haider, Carlos Cordeiro, and Edward W Knightly. 2019. Multi-user multi-stream mmWave WLANs with efficient path discovery and beam steering. *IEEE Journal on Selected Areas in Communications* 37, 12 (2019), 2744–2758.
[13] Ali Grami. 2015. *Introduction to digital communications*. Academic Press.
[14] Unsoo Ha, Junshan Leng, Alaa Khaddaj, and Fadel Adib. 2020. Food and Liquid Sensing in Practical Environments using RFIDs. In *17th {USENIX} Symposium on Networked Systems Design and Implementation ({NSDI} 20)*. 1083–1100.
[15] Daniel Halperin, Ben Greenstein, Anmol Sheth, and David Wetherall. 2010. Demystifying 802.11N Power Consumption. In *HotPower*.
[16] Haitham Hassanieh, Omid Abari, Michael Rodriguez, Mohammed Abdelghany, Dina Katabi, and Piotr Indyk. 2018. Fast millimeter wave beam alignment. In *Proceedings of the 2018 Conference of the ACM Special Interest Group on Data Communication*. 432–445.
[17] Dominique Henry, Jimmy GD Hester, Hervé Aubert, Patrick Pons, and Manos M Tentzeris. 2017. Long-range wireless interrogation of passive humidity sensors using van-atta cross-polarization effect and different beam scanning techniques. *IEEE Transactions on Microwave Theory and Techniques* 65, 12 (2017), 5345–5354.
[18] Elisabeth Ilie-Zudor, Zsolt Kemény, Fred Van Blommestein, László Monostori, and André Van Der Meulen. 2011. A survey of applications and requirements of unique identification systems and RFID techniques. *Computers in Industry* 62, 3 (2011), 227–252.
[19] Bryce Kellogg, Aaron Parks, Shyamnath Gollakota, Joshua R Smith, and David Wetherall. 2014. Wi-Fi backscatter: Internet connectivity for RF-powered devices. In *Proceedings of the 2014 ACM conference on SIGCOMM*. 607–618.
[20] Joongheon Kim and Andreas F Molisch. 2014. Fast millimeter-wave beam training with receive beamforming. *Journal of Communications and Networks* 16, 5 (2014), 512–522.
[21] John Kimionis, Apostolos Georgiadis, and Manos M Tentzeris. 2017. Millimeter-wave backscatter: A quantum leap for gigabit communication, RF sensing, and wearables. In *2017 IEEE MTT-S International Microwave Symposium (IMS)*. IEEE, 812–815.
[22] Bin Li, Zheng Zhou, Weixia Zou, Xuebin Sun, and Guanglong Du. 2012. On the efficient beam-forming training for 60GHz wireless personal area networks. *IEEE Transactions on Wireless Communications* 12, 2 (2012), 504–515.
[23] Zhuqi Li, Can Wu, Sigurd Wagner, James C Sturm, Naveen Verma, and Kyle Jamieson. 2021. REITS: Reflective Surface for Intelligent Transportation Systems. In *Proceedings of the 22nd International Workshop on Mobile Computing Systems and Applications*. 78–84.
[24] Robert J Mailloux. 2017. *Phased array antenna handbook*. Artech house.
[25] Mohammad H Mazaheri, Ali Abedi, and Omid Abari. 2018. Bringing mmWave Communications to Raspberry Pi. In *Proceedings of the 24th Annual International Conference on Mobile Computing and Networking*. 687–689.

[26] Mohammad H Mazaheri, Soroush Ameli, Ali Abedi, and Omid Abari. 2019. A millimeter wave network for billions of things. In *Proceedings of the ACM Special Interest Group on Data Communication*. 174–186.

[27] Yong Niu, Yong Li, Depeng Jin, Li Su, and Athanasios V Vasilakos. 2015. A survey of millimeter wave communications (mmWave) for 5G: opportunities and challenges. *Wireless networks* 21, 8 (2015), 2657–2676.

[28] Swadhin Pradhan, Eugene Chai, Karthikeyan Sundaresan, Lili Qiu, Mohammad A Khojastepour, and Sampath Rangarajan. 2017. Rio: A pervasive rfid-based touch gesture interface. In *Proceedings of the 23rd Annual International Conference on Mobile Computing and Networking*. 261–274.

[29] Swadhin Pradhan, Eugene Chai, Karthik Sundaresan, Sampath Rangarajan, and Lili Qiu. 2017. Konark: A RFID based system for enhancing in-store shopping experience. In *Proceedings of the 4th International on Workshop on Physical Analytics*. 19–24.

[30] Dinesh Ramasamy, Sriram Venkateswaran, and Upamanyu Madhow. 2012. Compressive tracking with 1000-element arrays: A framework for multi-Gbps mm wave cellular downlinks. In *2012 50th Annual Allerton Conference on Communication, Control, and Computing (Allerton)*. IEEE, 690–697.

[31] Sundeep Rangan, Theodore S Rappaport, and Elza Erkip. 2014. Millimeter-wave cellular wireless networks: Potentials and challenges. *Proc. IEEE* 102, 3 (2014), 366–385.

[32] Theodore S Rappaport, Shu Sun, Rimma Mayzus, Hang Zhao, Yaniv Azar, Kevin Wang, George N Wong, Jocelyn K Schulz, Mathew Samimi, and Felix Gutierrez. 2013. Millimeter wave mobile communications for 5G cellular: It will work! *IEEE access* 1 (2013), 335–349.

[33] Pei Ren, Xiuquan Qiao, Yakun Huang, Ling Liu, Calton Pu, Schahram Dustdar, and Jun-Liang Chen. 2020. Edge AR X5: An Edge-Assisted Multi-User Collaborative Framework for Mobile Web Augmented Reality in 5G and Beyond. *IEEE Transactions on Cloud Computing* (2020).

[34] Wonil Roh, Ji-Yun Seol, Jeongho Park, Byunghwan Lee, Jaekon Lee, Yungsoo Kim, Jaeweon Cho, Kyungwhoon Cheun, and Farshid Aryanfar. 2014. Millimeter-wave beamforming as an enabling technology for 5G cellular communications: Theoretical feasibility and prototype results. *IEEE communications magazine* 52, 2 (2014), 106–113.

[35] Swetank Kumar Saha, Yasaman Ghasempour, Muhammad Kumail Haider, Tariq Siddiqui, Paulo De Melo, Neerad Somanchi, Luke Zakrajsek, Arjun Singh, Roshan Shyamsunder, Owen Torres, et al. 2019. X60: A programmable testbed for wideband 60 ghz wlans with phased arrays. *Computer Communications* 133 (2019), 77–88.

[36] Swetank Kumar Saha, Tariq Siddiqui, Dimitrios Koutsonikolas, Adrian Loch, Joerg Widmer, and Ramalingam Sridhar. 2017. A detailed look into power consumption of commodity 60 GHz devices. In *WoWMoM*. 12–15.

[37] Stefano Savazzi, Monica Nicoli, and Vittorio Rampa. 2020. Federated learning with cooperating devices: A consensus approach for massive IoT networks. *IEEE Internet of Things Journal* 7, 5 (2020), 4641–4654.

[38] Aakash Sehrawat, T Anupriya Choudhury, and Gaurav Raj. 2017. Surveillance drone for disaster management and military security. In *2017 International Conference on Computing, Communication and Automation (ICCCA)*. IEEE, 470–475.

[39] E Sharp and M Diab. 1960. Van Atta reflector array. *IRE Transactions on Antennas and Propagation* 8, 4 (1960), 436–438.

[40] Vaibhav Singh, Susnata Mondal, Akshay Gadre, Milind Srivastava, Jeyanandh Paramesh, and Swarun Kumar. 2020. Millimeter-wave full duplex radios. In *Proceedings of the 26th Annual International Conference on Mobile Computing and Networking*. 1–14.

[41] Elahe Soltanaghaei, Akarsh Prabhakara, Artur Balanuta, Matthew Anderson, Jan M Rabaey, Swarun Kumar, and Anthony Rowe. 2021. Millimetro: mmWave retro-reflective tags for accurate, long range localization. In *Proceedings of the 27th Annual International Conference on Mobile Computing and Networking*. 69–82.

[42] Y Ming Tsang, Ada SY Poon, and Sateesh Addepalli. 2011. Coding the beams: Improving beamforming training in mmwave communication system. In *2011 IEEE Global Telecommunications Conference-GLOBECOM 2011*. IEEE, 1–6.

[43] Jue Wang, Haitham Hassanieh, Dina Katabi, and Piotr Indyk. 2012. Efficient and reliable low-power backscatter networks. *ACM SIGCOMM Computer Communication Review* 42, 4 (2012), 61–72.

[44] Jue Wang, Deepak Vasisht, and Dina Katabi. 2014. RF-IDraw: virtual touch screen in the air using RF signals. *ACM SIGCOMM Computer Communication Review* 44, 4 (2014), 235–246.

[45] Xiaoli Wang, Aakanksha Chowdhery, and Mung Chiang. 2017. Networked drone cameras for sports streaming. In *2017 IEEE 37th International Conference on Distributed Computing Systems (ICDCS)*. IEEE, 308–318.

[46] Wenfang Yuan, Simon MD Armour, and Angela Doufexi. 2015. An efficient and low-complexity beam training technique for mmWave communication. In *2015 IEEE 26th Annual International Symposium on Personal, Indoor, and Mobile Radio Communications (PIMRC)*. IEEE, 303–308.

[47] Jialiang Zhang, Xinyu Zhang, Pushkar Kulkarni, and Parameswaran Ramanathan. 2016. OpenMili: a 60 GHz software radio platform with a reconfigurable phased-array antenna. In *Proceedings of the 22nd Annual International Conference on Mobile Computing and Networking*. 162–175.

[48] Pengyu Zhang, Dinesh Bharadia, Kiran Joshi, and Sachin Katti. 2016. Hitchhike: Practical backscatter using commodity wifi. In *Proceedings of the 14th ACM Conference on Embedded Network Sensor Systems CD-ROM*. 259–271.

[49] Pengyu Zhang, Dinesh Bharadia, Kiran Joshi, and Sachin Katti. 2016. Hitchhike: Practical backscatter using commodity wifi. In *Proceedings of the 14th ACM Conference on Embedded Network Sensor Systems CD-ROM*. 259–271.

[50] Pengyu Zhang, Colleen Josephson, Dinesh Bharadia, and Sachin Katti. 2017. Freerider: Backscatter communication using commodity radios. In *Proceedings of the 13th International Conference on emerging Networking EXperiments and Technologies*. 389–401.

[51] Jia Zhao, Wei Gong, and Jiangchuan Liu. 2018. Spatial stream backscatter using commodity wifi. In *Proceedings of the 16th Annual International Conference on Mobile Systems, Applications, and Services*. 191–203.

[52] Guangxu Zhu, Yong Wang, and Kaibin Huang. 2019. Broadband analog aggregation for low-latency federated edge learning. *IEEE Transactions on Wireless Communications* 19, 1 (2019), 491–506.